



Published in final edited form as:

Invest Ophthalmol Vis Sci. 2006 October ; 47(10): 4513–4522. doi:10.1167/iovs.06-0404.

Bovine and Porcine Transscleral Solute Transport: Influence of Lipophilicity and the Choroid–Bruch’s Layer

Narayan P. S. Cheruvu¹ and Uday B. Kompella^{1,2}

¹Department of Pharmaceutical Sciences, University of Nebraska Medical Center, Omaha, Nebraska

²Department of Ophthalmology, University of Nebraska Medical Center, Omaha, Nebraska

Abstract

Purpose—To determine the influence of the choroid–Bruch’s layer and solute lipophilicity on in vitro transscleral drug permeability in bovine and porcine eyes.

Methods—The in vitro permeability of two VEGF inhibitory drugs, budesonide and celecoxib, which are lipophilic and neutral at physiologic pH, and of three marker solutes, ³H-mannitol (hydrophilic, neutral), sodium fluorescein (hydrophilic, anionic), and rhodamine 6G (lipophilic, cationic), were determined across freshly excised scleras, with or without the underlying choroid–Bruch’s layer. Select studies were performed using porcine sclera with and without choroid–Bruch’s layer. Neural retina was removed by exposure of the eyecup to isotonic buffer and wherever required, the retinal pigment epithelial (RPE) layer of the preparation was disrupted and removed by exposure to hypertonic buffer. Because of the poor solubility of celecoxib and budesonide, permeability studies were conducted with 5% wt/vol of hydroxypropyl- β -cyclodextrin (HP β CD). For other solutes, permeability studies were conducted, with and without HP β CD. Partitioning of the solutes into bovine sclera and choroid–Bruch’s layer was also determined.

Results—The calculated log (distribution coefficient) values were –2.89, –0.68, 2.18, 3.12, and 4.02 for mannitol, sodium fluorescein, budesonide, celecoxib, and rhodamine 6G, respectively. Removal of RPE was confirmed by transmission electron microscopy and differences in the transport of mannitol. The order of the permeability coefficients (P_{app}) across sclera and sclera–choroid–Bruch’s layers in bovine and porcine models was ³H-mannitol > fluorescein > budesonide > celecoxib > rhodamine 6G, with HP β CD, and ³H-mannitol > fluorescein > rhodamine 6G, without HP β CD. The presence of choroid–Bruch’s layer reduced the bovine scleral permeability by 2-, 8-, 16-, 36-, and 50-fold and porcine tissue permeability by 2-, 7-, 15-, 33-, and 40-fold, respectively, for mannitol, sodium fluorescein, budesonide, celecoxib, and rhodamine 6G. The partition coefficients measured in bovine tissues correlated positively with the log (distribution coefficient) and exhibited a trend opposite that of transport. The partition coefficient ratio of bovine choroid–Bruch’s layer to sclera was ~1, 1.5, 1.7, 2, and 3.5, respectively, for the solutes, as listed earlier.

Conclusions—The choroid–Bruch’s layer is a more significant barrier to drug transport than is sclera. It hinders the transport of lipophilic solutes, especially a cationic solute, more than

Copyright © Association for Research in Vision and Ophthalmology

Corresponding author: Uday B. Kompella, 985840 Nebraska Medical Center, Omaha, NE 68198-5840; ukompell@unmc.edu.

Presented in part at the annual meetings of the Association for Research in Vision and Ophthalmology, Fort Lauderdale, Florida, May 2003, May 2004, and May 2005.

Disclosure: N.P.S. Cheruvu, P; U.B. Kompella, Cerestar US, Inc. (F), P

hydrophilic solutes and in a more dramatic way than does sclera. The reduction in transport across this layer directly correlates with solute binding to the tissue. Understanding the permeability properties of sclera and underlying layers would be beneficial in designing better drugs for transscleral delivery.

Advances in cellular and molecular biology have shown that an elevation in vascular endothelial growth factor (VEGF) is a key contributor to vision-threatening diseases such as diabetic retinopathy and age-related macular degeneration.¹ To inhibit the expression and/or activity of VEGF, several pharmacological agents² including corticosteroids,³ nonsteroidal anti-inflammatory drugs,⁴ anti-VEGF antibodies, VEGF soluble receptors, and VEGF aptamers⁵ are being developed. It is noteworthy that a monoclonal VEGF antibody (Avastin; Genentech, South San Francisco, CA) and a VEGF aptamer (Macugen; Eye Tech, New York, NY) have been recently approved to inhibit angiogenesis associated with colorectal cancer and for the treatment of age-related macular degeneration, respectively. However, the bottleneck in the treatment of retinal angiogenic disorders as well as other diseases of the posterior segment is the delivery of adequate levels of drugs to the retina for prolonged periods.

The topical ocular route is inefficient in delivering adequate drug levels to the retina, and systemic modes of administration require high doses for delivering therapeutic concentrations, leading to systemic toxicity.⁶ Although intravitreal administration delivers adequate drug levels to the retina, repeated intravitreal injections as well as the surgical placement of intravitreal implants are associated with complications such as retinal detachment, endophthalmitis, and cataracts.⁷ Thus, there is a need for the development of alternative approaches for effective retinal drug delivery. Transscleral routes are now emerging as viable alternatives for retinal drug delivery. Studies over the past four decades have shown that the sclera is more permeable than the cornea⁸ and that various approaches, including particulate systems,^{3,5} episcleral implants,⁹ fibrin sealants,¹⁰ and collagen matrices,¹¹ can be used for delivering effective drug levels transsclerally in a sustained manner to the retina. Despite this promise, relatively little is known about the drug permeability properties of the sclera and the underlying layers.

In the transscleral route of drug entry, drug placed next to the sclera is expected to reach the retina primarily via transport across the sclera and underlying tissues including the choroid–Bruch’s layer and RPE. In all the earlier reports on transscleral drug transport, the solute permeability across the sclera has been reported. Also, the permeability-limiting nature of the RPE is well known.^{12–14} It is likely that the choroid layer containing Bruch’s membrane, located between the sclera and the RPE,¹⁵ can also affect the permeability of the drugs. There are no earlier reports on the influence of this layer on transscleral drug diffusion, although it is known that Bruch’s membrane thickens and the choroidal layer thins out with aging in the human eye.¹⁶

Our previous results demonstrate that celecoxib (a selective Cox-2 inhibitor) and budesonide (a corticosteroid) can inhibit VEGF expression in cell cultures.^{3,4,17} We have also demonstrated that transscleral sustained retinal delivery of celecoxib inhibits VEGF expression and vascular leakage in a diabetic rat model.¹⁷ Because of the promise of budesonide and celecoxib as therapeutic agents for inhibiting VEGF expression and other inflammatory mediators in disorders of the posterior segment, we chose these lipophilic, neutral molecules for use in the present study. Further, we assessed commonly used marker solutes, including mannitol (hydrophilic, neutral), sodium fluorescein (hydrophilic, anionic), and rhodamine 6G (R6G; lipophilic, cationic).

For investigating the effects of the choroid–Bruch’s layer on transscleral transport, we used bovine and porcine eyes in side-by-side diffusion chambers. The bovine eyes were used because freshly excised bovine eyes are readily available, and transport studies with the bovine eyes have been reported.¹⁸ The porcine eye, although limited in supply, resembles the human eye better in anatomic characteristics.¹⁹ The bovine eye, unlike the porcine eye, has a modified choroid called the choroid-tapetum, which enables night vision. The choroid layer in this report refers to the choroid–Bruch’s membrane combination with (bovine) or without (porcine) the tapetum.

Materials and Methods

Budesonide, R6G, and sodium fluorescein (NaFl) were purchased from Sigma-Aldrich (St. Louis, MO); celecoxib from Chem Pacific (Baltimore, MD); and [1-³H]-mannitol (10 Ci/mmol) and ³H-water (37 MBq/mmol) from American Radiolabeled Chemicals, Inc. (St. Louis, MO). Hydroxypropyl β cyclodextrin (HP β CD) was a gift from Cerestar US, Inc. (Hammond, IN). High performance liquid chromatography (HPLC) grade acetonitrile was obtained from Fisher Scientific (Philadelphia, PA) and tissue solubilizer (Solvable) from Perkin Elmer (Boston, MA).

Tissue Isolation

Freshly excised bovine eyes (Nebraska Beef, Omaha, NE; age of cows, 1–1.5 years) were used in most of the studies, and porcine eyes (J & J Meats, Omaha, NE; age of pigs: 6–8 months) were used in a few selected studies due to limited availability of porcine eyes. After the adherent muscle tissue was removed, the anterior segment of the eye was removed with a circumferential cut behind the limbus. The eye was cut into two halves along the *geometric axis*, a line joining the anterior pole (corneal center) and the posterior pole (center of the scleral curve), and the vitreous was removed. For performing transport experiments across the sclera–choroid–Bruch’s–RPE layer, neural retina was removed by exposing the eyecup to isotonic assay buffer at pH 7.4. To disrupt the RPE, the eyecups, devoid of neural retina, were filled with buffered hypertonic solution (5% wt/vol NaCl in assay buffer) and incubated for 2 to 3 minutes. After the treatment, the detached RPE was gently brushed off. This procedure was repeated thrice. Rectangular pieces (~1.5 × 1.5 cm) of the tissue containing the choroid layer and Bruch’s membrane along with the sclera were dissected from the equatorial region of the sclera. For measuring solute transport across the sclera, the choroid layer along with Bruch’s membrane was gently scraped off and removed.

Bovine Scleral Thickness Measurement

The thickness of sclera devoid of underlying layers was measured by placing the ultrasound pachymeter (DGH 500; DGH Technology, Inc., Exton, PA) at the limbus, equator, or optical nerve region.

Transmission Electron Microscopy

For determining the disruption and removal of the RPE layer after hypertonic solution treatment of the eyecup, the sclera–choroid–RPE tissues were fixed in 2.5% glutaraldehyde and 2% paraformaldehyde in Sorensen phosphate buffer. The tissue specimens were embedded in epoxy resin, and ultrathin (5 μ m) sections were observed using a transmission electron microscope (TEM; model 300, Philips/FEI, Briarcliff Manor, NY). TEM images of untreated tissue samples were also taken for comparison.

In Vitro Transscleral Transport Study

All transport studies were conducted with isotonic assay buffer (pH 7.4) with the following composition: NaCl (122 mM), NaHCO₃ (25 mM), MgSO₄ (1.2 mM), K₂HPO₄ (0.4 mM), CaCl₂ (1.4 mM), HEPES (10 mM), and glucose (10 mM). The isolated tissues were mounted in modified Ussing chambers (Naviclyte, Sparks, NV) with the episcleral side facing the donor chamber and the vitreous side facing the receiver chamber. The chambers were filled with equal volumes of assay buffer, with (donor side) or without (receiver side) the drug. In preparing the donor solutions of budesonide and celecoxib (100 μg/mL), 5% wt/vol HPβCD was used in assay buffer, to improve drug solubility. For comparative purposes, HPβCD at the same concentration was used with other solutes, including ³H-mannitol (1 μCi/mL and 10 μM unlabeled mannitol), sodium fluorescein (36.7 μg/mL), and R6G (100 μg/mL). To understand the tissue permeability properties in the absence of HPβCD, transscleral transport studies were conducted for ³H-mannitol, sodium fluorescein, and R6G without HPβCD. In Table 1, the physicochemical properties of the solutes are summarized.^{17,20,21} During the transport study, the bathing fluids were maintained at 37°C and pH 7.4 in 95% air-5% CO₂ aeration. At predetermined intervals (1, 2, 4, and 6 hours), 200 μL of sample was collected from the receiver side, and the lost volume was replaced with fresh assay buffer pre-equilibrated at 37°C. The drug levels were analyzed with either an HPLC assay (budesonide and celecoxib), a spectrofluorometric method (sodium fluorescein and R6G), or a liquid scintillation counter (³H-mannitol). The apparent permeability coefficient (P_{app}) was calculated with the following equation:

$$P_{app}=(dM/dt)/(A \cdot C_d)$$

In the equation, dM/dt is the slope of the linear region of the cumulative amount of the solute transported versus time plot, A is the area of the scleral surface (0.64 cm²) available for transport, and C_d is the initial donor drug concentration. Permeation data were corrected for dilution of the receiver solution with sample volume replenishment.

Hypertonic Treatment of the Eyecup and ³H-mannitol Permeability

The removal of RPE was further assessed by studying the transport of the paracellular marker ³H-mannitol across the sclera–choroid–Bruch's membrane–RPE. The permeability studies across the tissue were also performed in the presence of 0.5% EDTA, with and without hypertonic treatment, for comparison.

³H-mannitol and ³H-water Transport in the Presence of R6G

Transport of ³H-mannitol (1 μCi/mL) or ³H-water (1 μCi/mL) was measured in the presence of R6G, to determine whether binding of R6G to tissue reduces transscleral water movement and hydrophilic solute transport.

In Vitro Tissue Partitioning Studies

These studies were performed on all the solutes, to determine the relative affinity of the solute to the tissue compared with the assay buffer. For the partition studies, only bovine eyes were used. Approximately 100 mg of sclera or choroid–Bruch's layer was incubated with 0.5 mL solutions of each solute. Two concentrations of solutes differing by 100-fold were chosen for partition studies, to determine the effect of concentration on partitioning. Drug solutions were removed at the end of 1 or 6 hours, the tissues were washed with 1 mL of assay buffer and homogenized, and the drug concentrations in the homogenates were estimated. The tissue partition coefficients were estimated as the ratio of drug concentration

in the tissue to that in the buffer at the end of equilibration, presuming that 1 g of tissue is equivalent to 1 mL.

Solute Estimations

³H-mannitol—The concentration of ³H-mannitol was measured with a liquid scintillation counter (LS, 6000IC; Beckman Instruments, Irvine, CA). The concentration of ³H-mannitol for transport study samples and the supernatant samples in the partition study were estimated after the addition of a scintillation cocktail (Scintisafe; Fisher Scientific, Fair Lawn, NJ). The concentration of ³H-mannitol in the tissue pellet for the partition study was estimated by digesting the tissues (Solvable; Perkin Elmer) and estimating the activity after the addition of the scintillation cocktail.

Sodium Fluorescein and R6G—The concentration of sodium fluorescein and R6G for the transport study samples and the supernatant of the partition study were estimated with a fluorescence spectrophotometer (RF5000; Shimadzu, Columbia, MO). The wavelengths of excitation and emission were 480 nm and 510 nm for sodium fluorescein and 540 and 590 nm for R6G. The tissue pellets from the partition study were homogenized with 1 mL of buffer in a tissue tearer and centrifuged to remove the tissue debris. The concentration of the supernatant was estimated from the standards processed in a similar manner.

Estimation of Celecoxib and Budesonide—Concentrations of celecoxib and budesonide from the transport study and the supernatant from the partition study were estimated by using previously reported HPLC methods.^{20,22} For estimating the tissue pellet concentrations from the partition study, the tissue pellet was homogenized with 200 μ L of assay buffer in a tissue tearer, and the drugs were extracted using 2 mL of methylene chloride. Budesonide served as an internal standard for celecoxib and vice versa. The extract was transferred to a glass tube and evaporated in N₂. The solutes were reconstituted with 200 μ L of mobile phase, and 100 μ L of this reconstituted sample was injected (Plus Injector 717; Waters, Millipore, Bedford, MA) onto an HPLC column (100 Å, 5 μ m, C18, 25 cm; Microsorb; Varian, Inc., Palo Alto, CA). The standards were processed in similar manner. The mobile phase was maintained at a flow rate of 0.8 mL/min (616 pump; Waters). Celecoxib and budesonide were detected with a photodiode array detector (PDA 996; Waters) set at 250 nm. They were quantified with standards processed similarly.

Data Analysis

All data are expressed as the mean \pm SD, and comparison of the means was performed by using one-way analysis of variance (ANOVA) followed by the Tukey post hoc analysis (SPSS, ver. 8.0; SPSS, Chicago, IL). Statistical significance was set at $P < 0.05$.

Results

Bovine Scleral Thickness

The average thicknesses of the bovine sclera measured at the limbus, equator, and optic nerve regions are summarized in Table 2. For comparison purposes, literature-reported values for porcine,¹⁹ rabbit,²³ and human²⁴ scleras are also shown.

Transmission Electron Microscopy

TEM images of bovine and porcine scleral tissues, with and without hypertonic treatments are shown in Figure 1. Figure 1A shows the TEM images of the bovine and porcine eyecups, respectively, after removal of the neural retina by exposing it to isotonic assay buffer. At this stage, the choroid–Bruch's layer and RPE are intact. Figures 1B and 1D show TEM images

of the bovine and porcine eyecups, respectively, after hypertonic treatment. It is apparent that the RPE was removed from the supporting choroid–Bruch’s layer after hypertonic treatment. Figure 1C is porcine eyecup prior to any treatments.

Influence of Hypertonic Treatment on Bovine Scleral ^3H -mannitol Permeability

^3H -mannitol permeability ($4.27 \pm 0.83 \times 10^{-6}$ cm/s; $n = 6$) was lower across the sclera–choroid–Bruch’s–RPE than that across the sclera–choroid–Bruch’s layer obtained after hypertonic treatment ($7.26 \pm 0.62 \times 10^{-6}$). Further, the permeability coefficient of ^3H -mannitol across the sclera–choroid–Bruch’s layer–RPE after hypertonic treatment was similar to the permeability coefficient in the presence of a tight junction disrupter (0.5% EDTA; $7.05 \pm 1.12 \times 10^{-6}$), indicating functional absence of RPE layer after hypertonic treatment. This is further confirmed by the similar mannitol permeability across the sclera–choroid–Bruch’s layer and the EDTA-treated sclera–choroid–Bruch’s–RPE layer ($8.02 \pm 1.31 \times 10^{-6}$).

Bovine and Porcine Scleral Solute Transport in the Presence of $\text{HP}\beta\text{CD}$

The cumulative percentage of transport across the bovine and porcine sclera as well as the bovine and porcine sclera–choroid–Bruch’s layers were in the order (Fig. 2): ^3H -mannitol > sodium fluorescein > budesonide > celecoxib > R6G. The cumulative percentage of transport in the presence of the sclera–choroid–Bruch’s layer was lower than that in the presence of the sclera alone. The decrease (x -fold) in the transport of the solutes in the presence of the choroid–Bruch’s layer increased with increase in the lipophilicity. The decrease in the transport was approximately 2-, 8-, 16-, 36-, and 50-fold with bovine choroid–Bruch’s layer and 2-, 7-, 15-, 33-, and 40-fold with porcine choroid–Bruch’s layer, for mannitol, sodium fluorescein, budesonide, celecoxib, and R6G, respectively. Thus, the choroid–Bruch’s layer was more discriminating for lipophilic solutes and particularly for a positively charged lipophilic solute.

Bovine Scleral Permeability of ^3H -mannitol, Sodium Fluorescein, and R6G in the Absence of $\text{HP}\beta\text{CD}$

The solute permeabilities across the bovine sclera and the sclera–choroid–Bruch’s layer exhibited the same trend—that is, ^3H -mannitol > sodium fluorescein > R6G, even in the absence of $\text{HP}\beta\text{CD}$. However, the presence of $\text{HP}\beta\text{CD}$ reduced the permeabilities of ^3H -mannitol and sodium fluorescein (Fig. 3). The percentage decrease in permeability coefficients in the presence of $\text{HP}\beta\text{CD}$ were 42%, 50%, and 75% across sclera and 42%, 50%, and 77% across the sclera–choroid–Bruch’s preparation for mannitol, sodium fluorescein, and R6G, respectively.

Estimated Solute Permeabilities of Bovine and Porcine Choroid–Bruch’s Layers

The permeability coefficients for choroid–Bruch’s layer were derived by using the theory of “multilayer diffusion” using the following equation:

$$\frac{1}{P_{\text{app}}(B)} = \frac{1}{P_{\text{app}}(AB)} - \frac{1}{P_{\text{app}}(A)}$$

where $P_{\text{app}}(AB)$ is the permeability coefficient across the sclera–choroid–Bruch’s layer combination; $P_{\text{app}}(A)$ is the permeability coefficient across the sclera; $P_{\text{app}}(B)$ is the permeability coefficient across the choroid–Bruch’s layer; and $1/P_{\text{app}}$ for each layer represents the corresponding resistance offered by the tissue layer. Figure 4 shows the linear correlation of the log P_{app} to the log distribution (log D) coefficient in the bovine and

porcine sclera, sclera–choroid–Bruch’s layer, and choroid–Bruch’s layer. The derived permeabilities of the choroid–Bruch’s layer are compared with the experimental permeabilities of the sclera and sclera–choroid–Bruch’s layer in Table 3 (also summarizes other permeability data). A good correlation was observed between log D and the scleral and choroid–Bruch’s layer solute permeabilities for the bovine as well as the porcine model. The resistance offered by the bovine and porcine scleral and choroid–Bruch’s layers to the solute permeability is summarized in Table 3. Plots for correlation of permeabilities between bovine and porcine tissues for the sclera, sclera–choroid–Bruch’s layer, and choroid–Bruch’s layer are shown in Figure 5. The permeability coefficients for the five solutes correlated well between the two species, with the correlation coefficients for the sclera, sclera–choroid–Bruch’s layer, and choroid–Bruch’s layer being 0.9648, 0.9997, and 0.9999, respectively.

Influence of R6G on Bovine Scleral Transport of ^3H -mannitol and ^3H -water

The permeability of ^3H -water across the sclera and the sclera–choroid–Bruch’s preparation was similar in the presence and absence of R6G (Figs. 6A, 6B). However, the presence of R6G at two different concentrations, 100 and 200 $\mu\text{g}/\text{mL}$, significantly reduced the cumulative transport of ^3H -mannitol across the bovine sclera (from $10.53\% \pm 2.71\%$ to $5.4\% \pm 0.7\%$ and $4.75\% \pm 0.88\%$, respectively). For the sclera–choroid–Bruch’s layer, ^3H -mannitol transport decreased from $3.31\% \pm 0.91\%$ to $1.89\% \pm 0.50\%$ and $1.84\% \pm 0.18\%$, respectively, in the presence of 100 and 200 $\mu\text{g}/\text{mL}$ of R6G (Figs. 6C, 6D).

Bovine Tissue Partitioning

The tissue partition coefficients of solutes at the end of 6 hours are summarized in Table 4. The results did not differ significantly with incubation time or solute concentration. The choroid–Bruch’s layer partition coefficients were in the following order: R6G > celecoxib > budesonide > sodium fluorescein > ^3H -mannitol. The rank order of the sclera partition coefficients was similar. Except for ^3H -mannitol, the solute tissue partitioning coefficients were significantly higher in the choroid–Bruch’s layer than in the sclera. The partition coefficients of bovine choroid–Bruch’s layer were approximately 3.5-, 2-, 1.7-, and 1.5-fold higher for R6G, celecoxib, budesonide, and sodium fluorescein, respectively, compared with the coefficients of the sclera.

Discussion

Although several studies have been conducted to investigate transscleral transport, the physicochemical properties that influence solute transport across the sclera or the underlying choroid–Bruch’s layer have yet to be delineated. We have developed a tissue model for understanding the permeability characteristics of the choroid–Bruch’s layer without RPE and compared the effect of lipophilicity on the transport of molecules of similar size across this layer as well as the sclera.

Scleral permeabilities have been reported for the rabbit, bovine, porcine, and human species.^{8,18,25,26} The authors in these studies have concluded that the scleral permeability is dependent on the permeant molecular weight and permeant molecular radius. Ambati et al.,²⁵ using rabbit sclera, demonstrated that the molecular radius is a better predictor of scleral permeability than is the molecular weight. Among the solutes we investigated, four molecules have a very similar molecular radius (0.53–0.57 nm). According to previous studies in the literature, the permeabilities of these solutes should be close. However, we observed that despite similar molecular radii, these solutes exhibit different permeabilities, ranging from 3.33×10^{-6} cm/s for fluorescein to 0.91×10^{-6} cm/s for R6G in bovine sclera; and 3.46×10^{-6} cm/s for fluorescein and 0.96×10^{-6} cm/s for R6G in porcine sclera. These

apparent differences correlate well with the lipophilicity (Fig. 4). With molecules of similar radii, the permeability was higher for the more hydrophilic molecules than for the lipophilic ones. We have also investigated the permeability of mannitol, which is a molecule with a molecular weight of 180 and a smaller molecular radius of 0.43 nm. As expected from previous studies,^{8,18,25,27} we found the scleral permeability to be the highest for mannitol, most likely due to its lower molecular weight and radius. When fluorescein permeability across the sclera was compared with that of celecoxib (both molecules with same molecular radii) we saw a pronounced decrease in scleral transport with increasing lipophilicity. This effect was observed in bovine as well as porcine sclera. Using the data from a bovine study,¹⁸ we calculated the expected values for scleral permeability of all the solutes in our study by plotting the log permeabilities versus the molecular radius and fitting the result to a regression line. The reduction in permeabilities of sodium fluorescein, budesonide, celecoxib, and R6G when compared with mannitol was 15%, 18%, 15%, and 20%, respectively, based on molecular radius. Similarly, when the data from another study of rabbits²⁵ were used to perform the same calculations, a reduction of 6%, 7%, 6%, and 8% was obtained for sodium fluorescein, budesonide, celecoxib, and R6G, respectively. In this study, the observed percentage reduction for these solutes when compared with mannitol was 48%, 56%, 66%, and 86%, respectively, in the presence of HP β CD. Even in the absence of HP β CD, the observed percentage reduction for sodium fluorescein and R6G when compared with mannitol was 38% and 66%, respectively, clearly showing an influence of lipophilicity in addition to molecular size.

Although we used an air-lift system for mixing tissue-bathing fluids, another explanation of the observed results is unstirred water layers, which can reduce the permeability of poorly soluble solutes more than that of the more soluble solutes.²⁸ Even though the unstirred water layer in the human intestine, as opposed to in vitro systems, is estimated to be thinner due to peristaltic movements and constant mixing,²⁹ the thickness of this layer is uncertain in the subconjunctival space. In select studies, we performed transport studies with a small (molecular weight = 266; molecular radius = 0.47 nm), hydrophilic (log $D = -2.02$) and more soluble (500 mg/mL in water) β -blocker, atenolol, without HP β CD across the bovine sclera and sclera–choroid–Bruch's layer (Table 3). We observed that the permeabilities of atenolol across both bovine sclera [$(8.90 \pm 1.02) \times 10^{-6}$ cm/s] and sclera–choroid–Bruch's layer [$(4.24 \pm 0.75) \times 10^{-6}$ cm/s] are significantly higher than the corresponding data for sodium fluorescein and R6G but lower than that of mannitol. This finding is consistent with the dependence of transport on lipophilicity, as discussed earlier.

There is another factor that should be taken into consideration. We have two neutral (celecoxib and budesonide) and two charged (fluorescein and R6G) molecules of similar molecular radius in our studies. We found the permeability of sodium fluorescein (negatively charged) to be the highest and that of R6G (positively charged) to be the lowest in this group. It has been observed previously that the sclera is more permeable to negatively charged solutes than to positively charged solutes.¹⁸ Thus, in addition to lipophilicity, charge could also determine the scleral permeability for molecules of similar radii. Though no definite conclusions can be made about the effect of charge on scleral permeability because of the small number of molecules tested in this study, the trend indicates greater permeability for negatively charged solutes compared with positively charged ones.

Sclera is a collagenous tissue made up of an intercrossed matrix of collagen fibers. In addition to collagen, the scleral tissue is rich in proteoglycans and mucopolysaccharides. These proteoglycans have surface glycosaminoglycan groups that are negatively charged under physiological conditions.³⁰ Thus, scleral matrix can have an overall negative charge at the physiological pH. The binding of positively charged R6G to scleral collagen and other components of the scleral matrix, may have contributed, at least in part, to the low transport

of this molecule. When Maurice and Polgar¹⁸ first determined the scleral permeability, they also observed permeability differences between anionic and cationic dyes across the bovine sclera, with the permeability of anionic dyes being more than that of cationic dyes of similar molecular weight. With human sclera, Cruysberg et al.,³¹ reported that the permeability of the highly lipophilic R6G is lower than that of sodium fluorescein.

Prior studies primarily investigated transport across the sclera alone. We have for the first time elucidated the influence of underlying layers. In bovine as well as porcine tissues, the choroid–Bruch’s layer reduced the transport of all solutes, with the barrier property increasing with solute lipophilicity. The trend of decreasing permeability with increasing lipophilicity with molecules of similar radii is more steep for the sclera–choroid–Bruch’s layer when compared with sclera alone. Our tissue-partitioning studies showed a trend for increased partitioning into the sclera and choroid–Bruch’s layer with increasing lipophilicity. This partitioning may be reflective of binding interactions that are limiting the drug transport. Binding interactions can reduce the diffusion of molecules in a medium. Anomalous (non-Fickian) diffusion of solutes in biological systems has been widely reported.^{32,33} This anomalous diffusion is in part due to binding interactions of the solutes with the various proteins and other constituents. When a solute binds to the matrix, the diffusion coefficient D , is expected to be of the order $D/(1 + K)$, where K is the association constant. K in the range of 10 to 100 can drastically affect the overall diffusion.³⁴ It has been shown with collagen-based drug delivery systems that the release rate of the active agent from the hydrogel matrix, which is diffusion controlled, is reduced by the binding and electrostatic interactions.³⁵

The choroid, a part of the vascular tunic of the eye, supplies blood to the outer two-thirds of the retina.³⁶ The choroid is also made up of collagen and has properties of a connective tissue. Similar to the sclera, the choroid can be imagined as a matrix. The important differences between the sclera and choroid include the greater cellular content as well as the melanin content of the latter.³⁶ The permeability rank order, although similar across the sclera and the sclera–choroid–Bruch’s layers, the choroid–Bruch’s layer generally offers greater resistance than does the sclera (Table 3). The presence of melanin in the choroid can provide additional binding sites, especially for lipophilic and cationic solutes.³⁷ Possibly due to the presence of melanin and lipidic plasma membranes of endothelial cells, there is greater binding of the lipophilic drugs to the choroid–Bruch’s layer (Table 4), resulting in greater resistance to solute permeability than in the sclera. The choroid–Bruch’s layer could be even more formidable a barrier *in vivo*, due to the rapid blood flow, which can potentially remove solutes before they reach the retina.³⁸

In a previous study examining the effect of lipophilicity of drugs on transport across the choroid–RPE, Pitkanen et al.¹² observed a higher transport for lipophilic molecules ($\log D$ of 0.03–1.59) compared with the most hydrophilic, atenolol ($\log D$ of -1.77). However, no significant differences were seen within the lipophilic ($\log D$ 0.03–1.59) or hydrophilic ($\log D$ -0.07 to -1.77) solutes. Further, they observed higher lag times with the more lipophilic solutes. It is, however, not clear from their study whether the choroid–Bruch’s layer or the RPE is the major barrier for hydrophilic drugs. Using the sclera–choroid–Bruch’s–RPE preparation, we observed that the choroid–Bruch’s layer offers lower resistance to mannitol transport than does the sclera and RPE (Table 3). This can be explained on the basis of a thick sclera, lack of preferential binding of mannitol to choroid–Bruch’s layer, and the presence of tight junctions in the RPE cell monolayer. However, this scenario may be entirely different with solutes of greater lipophilicity. Our results suggest that qualitative transport across the choroid–Bruch’s layer behaves in a fashion similar to the transport across the sclera, differing only in magnitude, with the former being a more significant barrier for lipophilic solutes.

It has been reported that the transport across the choroid is greatly hindered due to the age-related changes in the human Bruch's membrane.^{16,39–41} Hillenkamp et al.,¹⁶ have observed the age-related decrease in hydraulic conductivity and taurine transport across the choroid–Bruch's layer in humans. Also, they have seen that in the human preparations, laser ablation of the Bruch's membrane⁴⁰ led to an increase in the diffusion across the choroid normalized to the thickness, indicating that the aged Bruch's membrane is a major barrier to transport. However, when they used bovine choroid–Bruch's layer samples obtained from cows aged 18 to 24 months, they did not observe the same increase in diffusion with the ablation of Bruch's membrane. In their bovine samples, with or without Bruch's membrane, taurine transport and hydraulic conductivity were similar.¹⁶ Our tissue preparation of sclera–choroid combination contained the Bruch's membrane. Although the cows used in our study (12–18 months) are of an age similar to the ones used in the previous study, we cannot comment on whether the reduction in transport due to the presence of the choroid–Bruch's layer is contributed by the choroid alone with the solutes used in this study.

For mannitol, sodium fluorescein, and R6G, we performed our studies with or without HP β CD. An interesting observation is that the presence of HP β CD reduced the transport of all three solutes. The decrease in transport was the highest for R6G (Table 3), possibly due to its better binding to the lipophilic interior of HP β CD. Such interactions as well as physical obstruction of pores by aggregates⁴² or monomers of HP β CD, which is a larger molecule present at greater concentrations compared with the permeating solutes, may reduce the primarily pore-based transport of solutes across scleral tissue. Further, we observed that R6G reduced the transport of ³H-mannitol but not ³H-water (Fig. 6), possibly by coating sclera/tissue pores by binding and effectively reducing the dimensions or hydrophilicity of the pores.

Heretofore, transport studies across the choroid–Bruch's layer^{16,41} or the choroid–RPE¹² have been performed by isolating these layers from the sclera. The choroid as well as the RPE are delicate, and isolating them from the sclera without any damage is technically demanding. Our model provides an in vitro system in which the transport properties of the intact choroid–Bruch's layer can be examined. The sclera acts as a supporting membrane to the choroid, and thus the transport across these two layers is closer to the actual physiology. By using the resistances in series law, it is possible to calculate the resistance of the choroidal layer, which we have done in this study. For removing the RPE we used buffered hypertonic saline (5% wt/vol) which is used in nasal irrigation.⁴³ This technique is simple and ensures removal of the RPE to study the transport properties of the sclera–choroid–Bruch's layer preparation.

Our studies indicate that the choroid–Bruch's layer is a significant barrier for transscleral delivery of drugs. If the choroid is the intended target for drug delivery by the transscleral route, hydrophilic and anionic drugs would have greater delivery across the sclera than would the lipophilic and cationic molecules. Thus, for treatment of such conditions as choroidal neovascularization, greater levels of free drug in the choroid can be achieved by designing hydrophilic drugs compared with lipophilic ones. Lipophilic and positively charged solutes may form a slow-release depot in the choroid–Bruch's layer. If the retina is the intended target, there is a further reduction in drug transport because of the presence of the choroid–Bruch's layer and RPE. The choroid–Bruch's layer, as observed in this study, allows greater permeability of hydrophilic and anionic solutes. When the RPE layer is also included, the design considerations are not simple, and no clear dependence of retinal delivery on lipophilicity is observed.⁴⁴ In addition, because of the cellular monolayer nature of the RPE, active transport processes⁴⁵ should be taken into consideration for effective drug design that can provide higher drug levels to the retina.

Conclusions

Hypertonic treatment of the eyecup effectively removes the neural retina and the RPE. For small molecules of similar radii, the transscleral and transchoroidal transport is affected by the lipophilicity of the molecule, with the transport being higher for hydrophilic molecules than for lipophilic ones and greater for negatively charged molecules than for positive ones. The choroid–Bruch’s layer binds lipophilic drugs preferentially and is a greater barrier for the transport of lipophilic molecules than is the sclera. In delivering small-molecule drugs transsclerally to the choroid or the retina, the lipophilicity and the charge must thus be taken into consideration. The bovine eye, despite the presence of a modified choroid (tapetum), behaves similarly to the porcine model with respect to transscleral transport for the solutes assessed. Similar thicknesses of bovine and porcine scleras in the equatorial region may be one reason for the observed similarities.

Acknowledgments

Supported by National Institute of Digestive and Kidney Disease Grant DK064172 (UBK), National Eye Institute Grant EY013842 (UBK), and a UNMC graduate fellowship (NPSC).

The authors thank Aniruddha Amrite for valuable contributions in the preparation of the manuscript, especially the Discussion section, and Tom Bargar (University of Nebraska Medical Center [UNMC] Electron Microscopy Core Facility) for help with transmission electron microscopy.

References

1. Adamis AP, Miller JW, Bernal MT, et al. Increased vascular endothelial growth factor levels in the vitreous of eyes with proliferative diabetic retinopathy. *Am J Ophthalmol*. 1994; 118:445–450. [PubMed: 7943121]
2. Speicher MA, Danis RP, Criswell M, Pratt L. Pharmacologic therapy for diabetic retinopathy. *Expert Opin Emerg Drugs*. 2003; 8:239–250. [PubMed: 14610924]
3. Kompella UB, Bandi N, Ayalasonmayajula SP. Subconjunctival nano- and microparticles sustain retinal delivery of budesonide, a corticosteroid capable of inhibiting VEGF expression. *Invest Ophthalmol Vis Sci*. 2003; 44:1192–1201. [PubMed: 12601049]
4. Ayalasonmayajula SP, Kompella UB. Celecoxib, a selective cyclooxygenase-2 inhibitor, inhibits retinal vascular endothelial growth factor expression and vascular leakage in a streptozotocin-induced diabetic rat model. *Eur J Pharmacol*. 2003; 458:283–289. [PubMed: 12504784]
5. Carrasquillo KG, Ricker JA, Rigas IK, Miller JW, Gragoudas ES, Adamis AP. Controlled delivery of the anti-VEGF aptamer EYE001 with poly(lactic-co-glycolic)acid microspheres. *Invest Ophthalmol Vis Sci*. 2003; 44:290–299. [PubMed: 12506087]
6. Maurice D. Review: practical issues in intravitreal drug delivery. *J Ocul Pharmacol Ther*. 2001; 17:393–401. [PubMed: 11572470]
7. Ambati J, Adamis AP. Transscleral drug delivery to the retina and choroid. *Prog Retin Eye Res*. 2002; 21:145–151. [PubMed: 12062532]
8. Edelhauser HF, Maren TH. Permeability of human cornea and sclera to sulfonamide carbonic anhydrase inhibitors. *Arch Ophthalmol*. 1988; 106:1110–1115. [PubMed: 3401140]
9. Kato A, Kimura H, Okabe K, Okabe J, Kunou N, Ogura Y. Feasibility of drug delivery to the posterior pole of the rabbit eye with an episcleral implant. *Invest Ophthalmol Vis Sci*. 2004; 45:238–244. [PubMed: 14691179]
10. Simpson AE, Gilbert JA, Rudnick DE, Geroski DH, Aaberg TM Jr, Edelhauser HF. Transscleral diffusion of carboplatin: an in vitro and in vivo study. *Arch Ophthalmol*. 2002; 120:1069–1074. [PubMed: 12149061]
11. Gilbert JA, Simpson AE, Rudnick DE, Geroski DH, Aaberg TM Jr, Edelhauser HF. Transscleral permeability and intraocular concentrations of cisplatin from a collagen matrix. *J Control Release*. 2003; 89:409–417. [PubMed: 12737843]

12. Pitkanen L, Ranta VP, Moilanen H, Urtti A. Permeability of retinal pigment epithelium: effects of permeant molecular weight and lipophilicity. *Invest Ophthalmol Vis Sci.* 2005; 46:641–646. [PubMed: 15671294]
13. Steuer H, Jaworski A, Stoll D, Schlosshauer B. In vitro model of the outer blood-retina barrier. *Brain Res Brain Res Protoc.* 2004; 13:26–36. [PubMed: 15063838]
14. Toimela T, Maenpaa H, Mannerstrom M, Tahti H. Development of an in vitro blood-brain barrier model-cytotoxicity of mercury and aluminum. *Toxicol Appl Pharmacol.* 2004; 195:73–82. [PubMed: 14962507]
15. Hogan, JMAJ.; Weddell, JE. *Histology of the Human Eye.* Philadelphia: WB Saunders; 1971.
16. Hillenkamp J, Hussain AA, Jackson TL, Cunningham JR, Marshall J. The influence of path length and matrix components on ageing characteristics of transport between the choroid and the outer retina. *Invest Ophthalmol Vis Sci.* 2004; 45:1493–1498. [PubMed: 15111607]
17. Amrite AC, Ayalasomayajula SP, Cheruvu NP, Kompella UB. Single periocular injection of celecoxib-PLGA microparticles inhibits diabetes-induced elevations in retinal PGE₂, VEGF, and vascular leakage. *Invest Ophthalmol Vis Sci.* 2006; 47:1149–1160. [PubMed: 16505053]
18. Maurice DM, Polgar J. Diffusion across the sclera. *Exp Eye Res.* 1977; 25:577–582. [PubMed: 590384]
19. Olsen TW, Sanderson S, Feng X, Hubbard WC. Porcine sclera: thickness and surface area. *Invest Ophthalmol Vis Sci.* 2002; 43:2529–2532. [PubMed: 12147580]
20. Martin TM, Bandi N, Shulz R, Roberts CB, Kompella UB. Preparation of budesonide and budesonide-PLA microparticles using supercritical fluid precipitation technology. *AAPS Pharm Sci Tech.* 2002; 3:E18.
21. Reddy MN, Rehana T, Ramakrishna S, Chowdhary KP, Diwan PV. Beta-cyclodextrin complexes of celecoxib: molecular-modeling, characterization, and dissolution studies. *AAPS Pharm Sci.* 2004; 6:E7.
22. Ayalasomayajula SP, Kompella UB. Retinal delivery of celecoxib is several-fold higher following subconjunctival administration compared to systemic administration. *Pharm Res.* 2004; 21:1797–1804. [PubMed: 15553225]
23. Prince, JH.; Eglitis, I.; Ruskell, GL. *Anatomy and Histology of the Eye and Orbit in Domestic Animals.* Springfield, IL: Charles C Thomas; 1960. The rabbit; p. 260-293.
24. Olsen TW, Aaberg SY, Geroski DH, Edelhauser HF. Human sclera: thickness and surface area. *Am J Ophthalmol.* 1998; 125:237–241. [PubMed: 9467451]
25. Ambati J, Canakis CS, Miller JW, et al. Diffusion of high molecular weight compounds through sclera. *Invest Ophthalmol Vis Sci.* 2000; 41:1181–1185. [PubMed: 10752958]
26. Amaral J, Fariss RN, Campos MM, et al. Transscleral-RPE permeability of PEDF and ovalbumin proteins: implications for subconjunctival protein delivery. *Invest Ophthalmol Vis Sci.* 2005; 46:4383–4392. [PubMed: 16303924]
27. Unlu N, Robinson JR. Scleral permeability to hydrocortisone and mannitol in the albino rabbit eye. *J Ocul Pharmacol Ther.* 1998; 14:273–281. [PubMed: 9671435]
28. Hidalgo IJ, Hillgren KM, Grass GM, Borchardt RT. Characterization of the unstirred water layer in Caco-2 cell monolayers using a novel diffusion apparatus. *Pharm Res.* 1991; 8:222–227. [PubMed: 2023871]
29. Avdeef A, Nielsen PE, Tsinman O. PAMPA: a drug absorption in vitro model 11. Matching the in vivo unstirred water layer thickness by individual-well stirring in microtitre plates. *Eur J Pharm Sci.* 2004; 22:365–374. [PubMed: 15265506]
30. Watson PG, Young RD. Scleral structure, organisation and disease: a review. *Exp Eye Res.* 2004; 78:609–623. [PubMed: 15106941]
31. Cruysberg LP, Nuijts RM, Geroski DH, Koole LH, Hendrikse F, Edelhauser HF. In vitro human scleral permeability of fluorescein, dexamethasone-fluorescein, methotrexate-fluorescein and rhodamine 6G and the use of a coated coil as a new drug delivery system. *J Ocul Pharmacol Ther.* 2002; 18:559–569. [PubMed: 12537682]
32. Wachsmuth M, Waldeck W, Langowski J. Anomalous diffusion of fluorescent probes inside living cell nuclei investigated by spatially-resolved fluorescence correlation spectroscopy. *J Mol Biol.* 2000; 298:677–689. [PubMed: 10788329]

33. Bacia K, Schwille P. A dynamic view of cellular processes by in vivo fluorescence auto- and cross-correlation spectroscopy. *Methods*. 2003; 29:74–85. [PubMed: 12543073]
34. Wallace DG, Rosenblatt J. Collagen gel systems for sustained delivery and tissue engineering. *Adv Drug Deliv Rev*. 2003; 55:1631–1649. [PubMed: 14623405]
35. Singh MP, Stefko J, Lumpkin JA, Rosenblatt J. The effect of electrostatic charge interactions on release rates of gentamicin from collagen matrices. *Pharm Res*. 1995; 12:1205–1210. [PubMed: 7494835]
36. Hogan, J. *Histology of the Human Eye*. Philadelphia: WB Saunders; 1971.
37. Zane PA, Brindle SD, Gause DO, O’Buck AJ, Raghavan PR, Tripp SL. Physicochemical factors associated with binding and retention of compounds in ocular melanin of rats: correlations using data from whole-body autoradiography and molecular modeling for multiple linear regression analyses. *Pharm Res*. 1990; 7:935–941. [PubMed: 2235893]
38. Robinson MR, Lee SS, Kim H, et al. A rabbit model for assessing the ocular barriers to the transscleral delivery of triamcinolone acetonide. *Exp Eye Res*. 2006; 82:479–487. [PubMed: 16168412]
39. Moore DJ, Hussain AA, Marshall J. Age-related variation in the hydraulic conductivity of Bruch’s membrane. *Invest Ophthalmol Vis Sci*. 1995; 36:1290–1297. [PubMed: 7775106]
40. Starita C, Hussain AA, Patmore A, Marshall J. Localization of the site of major resistance to fluid transport in Bruch’s membrane. *Invest Ophthalmol Vis Sci*. 1997; 38:762–767. [PubMed: 9071230]
41. Hussain AA, Rowe L, Marshall J. Age-related alterations in the diffusional transport of amino acids across the human Bruch’s-choroid complex. *J Opt Soc Am A Opt Image Sci Vis*. 2002; 19:166–172. [PubMed: 11778720]
42. Loftsson T, Masson M, Brewster ME. Self-association of cyclodextrins and cyclodextrin complexes. *J Pharm Sci*. 2004; 93:1091–1099. [PubMed: 15067686]
43. Tomooka LT, Murphy C, Davidson TM. Clinical study and literature review of nasal irrigation. *Laryngoscope*. 2000; 110:1189–1193. [PubMed: 10892694]
44. Cheruvu CPS, Ayalasomayajula SP, Kompella UB. Retinal delivery of sodium fluorescein, budesonide, and celecoxib following subconjunctival injection. *Drug Delivery Tech*. 2003; 3(6): 62–67.
45. Aukunuru JV, Sunkara G, Bandi N, Thoreson WB, Kompella UB. Expression of multidrug resistance-associated protein (MRP) in human retinal pigment epithelial cells and its interaction with BAPSG, a novel aldose reductase inhibitor. *Pharm Res*. 2001; 18:565–572. [PubMed: 11465409]

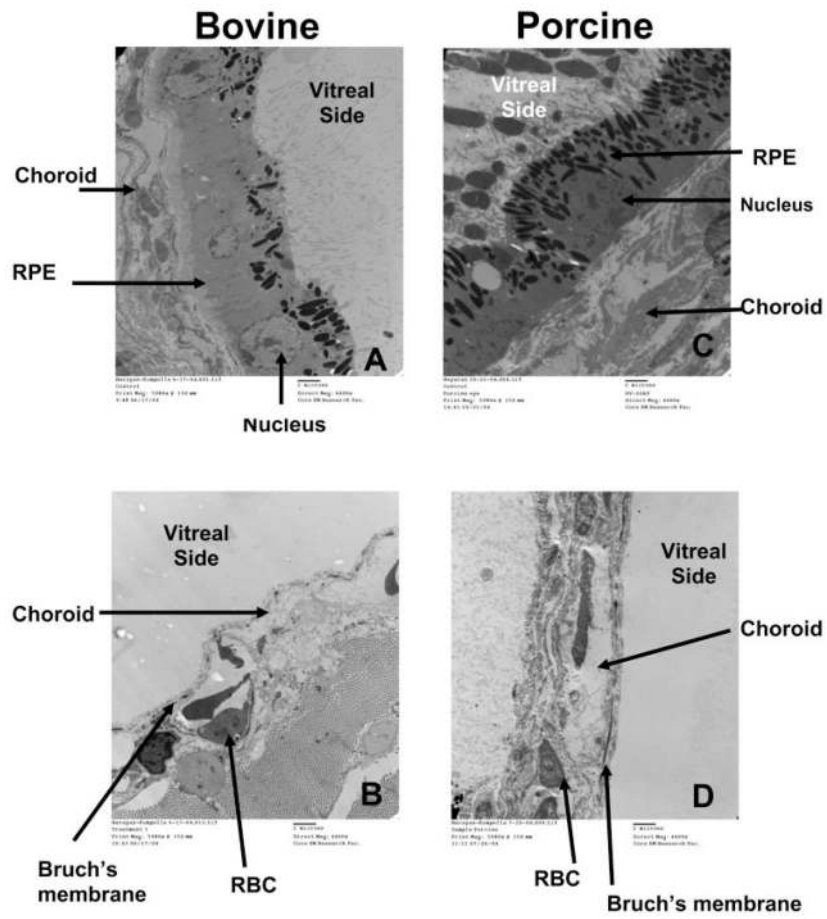


Figure 1. TEM image of the bovine eyecup after assay buffer treatment and (A) before and (B) after hypertonic treatment. TEM image of the porcine eyecup (C) before any treatment and (D) after assay buffer and hypertonic treatment. Hypertonic treatment removed the RPE layer in both the bovine and porcine tissues. Bar, 2 μ m.

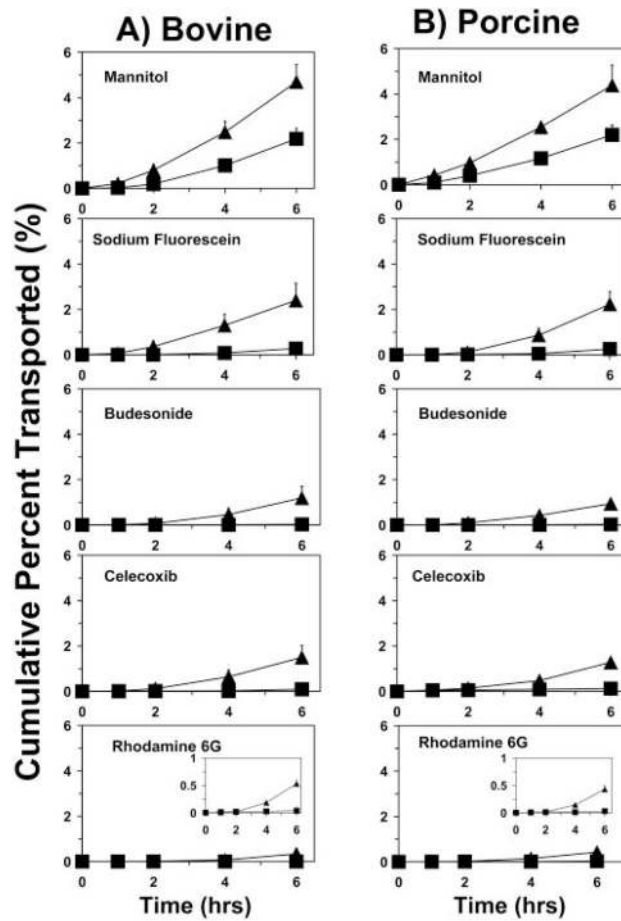


Figure 2. Cumulative percentage transport of various solutes across the sclera and the sclera-choroid-Bruch's layer in bovine (*left*) and porcine (*right*) models. All donor solutions contained 5% HP β CD, which was required for solubilizing some of the solutes used. (\blacktriangle) Sclera; (\blacksquare) sclera-choroid-Bruch's layer. Data are expressed as the mean \pm SD ($n = 6$).

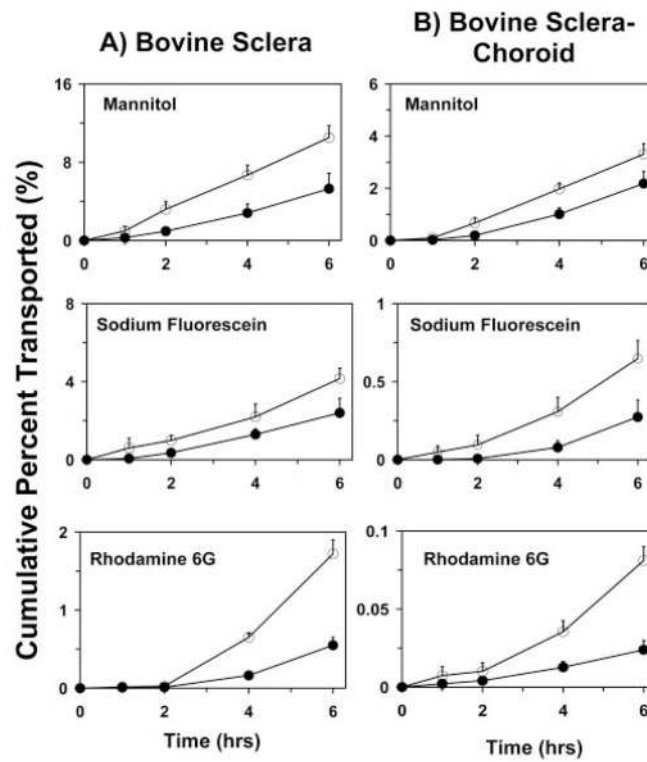


Figure 3. Cumulative percentage transport of mannitol, sodium fluorescein, and R6G, with (●) and without (○) 5% HPβCD across bovine sclera and bovine sclera-choroid-Bruch's layer. Data are expressed as the mean ± SD ($n = 6$).

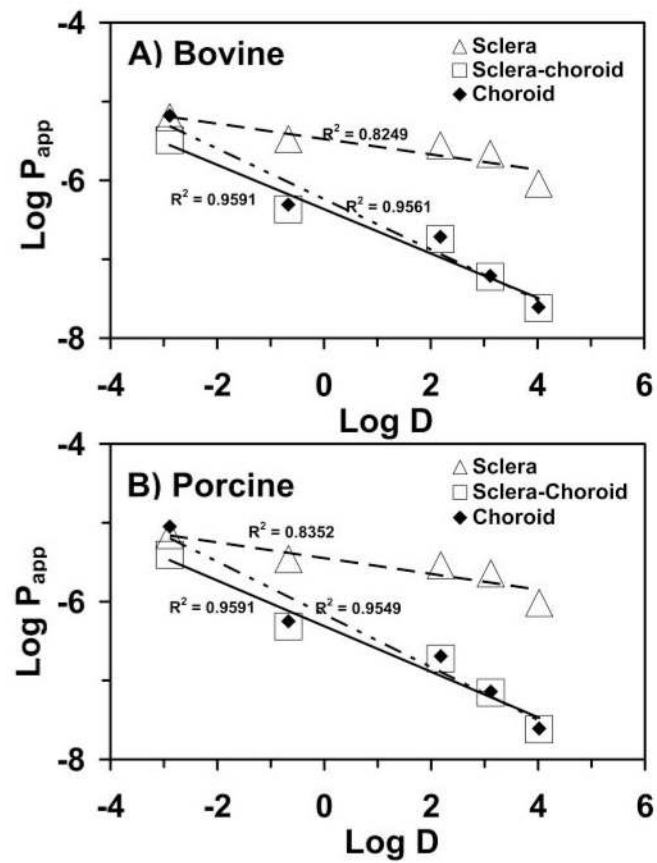


Figure 4. Correlation of solute permeability coefficients across (A) bovine and (B) porcine tissues with log (distribution coefficients) data. Results are expressed as the mean ($n = 6$).

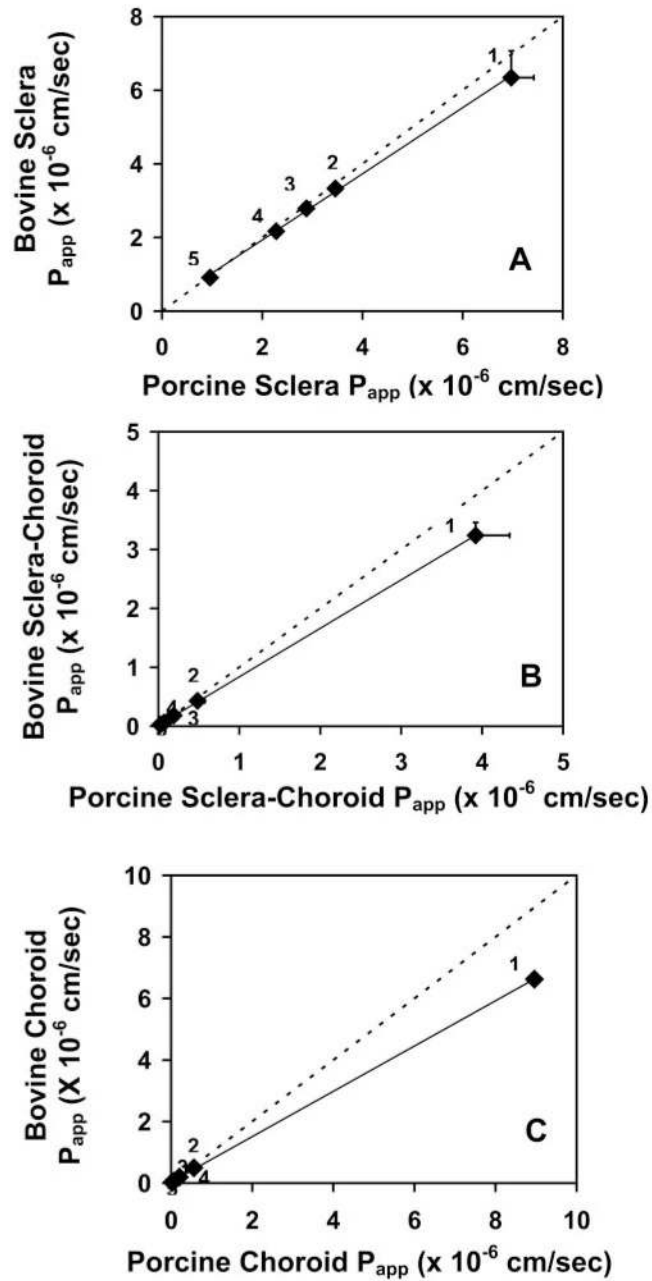


Figure 5. Correlation of solute permeability coefficients between porcine and bovine models for (A) sclera, (B) sclera-choroid-Bruch's layer, and (C) choroid-Bruch's layer. Permeabilities of (1) mannitol, (2) sodium fluorescein, (3) budesonide, (4) celecoxib, (5) and R6G were compared. Data are expressed as the mean \pm SD ($n = 6$). *Dashed line*: the trend line for 1:1 relationship.

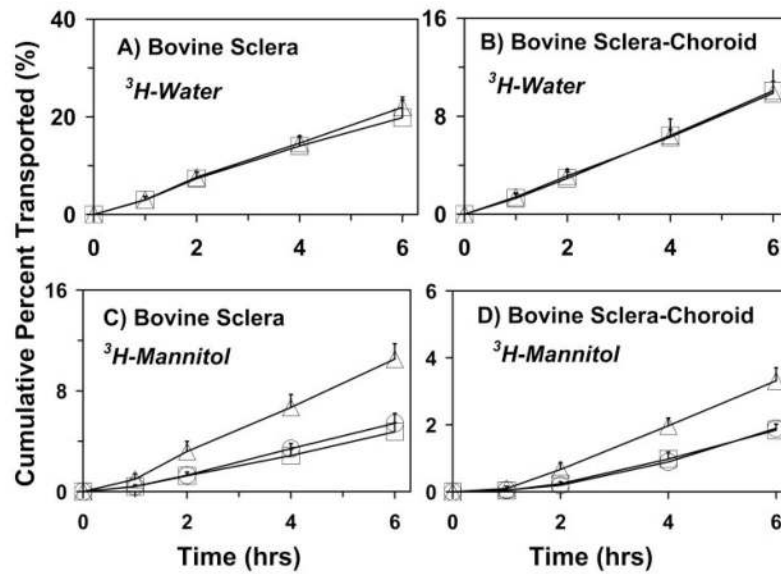


Figure 6. Influence of R6G on the transport of ^3H -water (A, B) and ^3H -mannitol (C, D) across bovine sclera (A, C) and sclera-choroid-Bruch's layer (B, D). Data are expressed as the mean \pm SD ($n = 6$). (Δ) 0 $\mu\text{g}/\text{mL}$; (\circ) 100 $\mu\text{g}/\text{mL}$; (\square) 200 $\mu\text{g}/\text{mL}$ of R6G. Only 0 and 200 $\mu\text{g}/\text{mL}$ of R6G were assessed for water transport.

Table 1

Physicochemical Properties of the Solutes

Solute	Molecular Weight	Molecular Radius (nm)	Log <i>D</i> *	Log <i>D</i>	Solubility (mg/mL in H ₂ O at 25°C)	pKa	Hydrogen Acceptors (<i>n</i>)	Hydrogen Donors (<i>n</i>)	Charge at pH 7.4
Mannitol	182.17	0.42	-2.89		1000	13.28, 2.52	6	6	Neutral
Sodium fluorescein (NaFl)	376.3	0.53	-0.68	-0.99	600	9.12, 0.38	5	2	Anionic (2)
Budesonide	430.53	0.55	2.18	3.20	0.02	14.39, 2.65	6	2	Neutral
Celecoxib	381.37	0.53	3.12	3.79	0.002	8.83, 0.80	1	3	Neutral
Rhodamine 6G	479.02	0.57	4.02		0.5	None, 4.87	4	1	Cationic (1)

Solubility [17,20,21] data were obtained from the literature. Molecular radius was calculated using the Stokes-Einstein equation. pKa (acidic group, basic group) and log *D** were obtained using Pallas 3.1.1 software (CompuDrug International, Inc., San Francisco, CA). Octanol-water (PBS, pH 7.4) partition coefficients (log *D*) were determined at 37°C by using the shake flask method for sodium fluorescein, budesonide, and celecoxib.

Table 2

Comparison of the Thickness of Human, Bovine, and Porcine Scleras

Tissue	Bovine	Porcine¹⁹	Rabbit²³	Human²⁴
Limbus	920 ± 60	800		530
Equator	646 ± 43	560	200	390
Optic nerve region	>1000	1000–1200		900–1000

Data are expressed as the mean ± SD (μm) of scleral thickness in $n = 3$ eyes. The thickness in the equator region was significantly lower than that in the limbus. The thickness in optic nerve region exceeded the limits of measurement with a pachymeter.

Table 3
Permeability Coefficients ($\times 10^{-6}$ cm/s) of the Solutes across Bovine and Porcine Ocular Tissues

Solute	Treatment	Bovine			Porcine		
		Sclera	Sclera-Choroid	Choroid	Sclera	Sclera-Choroid	Choroid
Mannitol	With HP β CD	6.34 \pm 0.73 (51)	3.24 \pm 0.22	6.62 (49)	6.97 \pm 0.45 (52)	3.92 \pm 0.42	6.14 (48)
	Without HP β CD	10.99 \pm 2.05 (66)	5.61 \pm 0.62	21.34 (34)	—	—	—
Atenolol	Without HP β CD	8.90 \pm 1.02 (48)	4.24 \pm 0.75	8.09 (52)	—	—	—
	With HP β CD	3.33 \pm 0.15 (13)	0.43 \pm 0.02	0.49 (87)	3.46 \pm 0.12 (11)	0.48 \pm 0.09	0.43 (89)
Budesonide	Without HP β CD	6.77 \pm 1.53 (12)	0.87 \pm 0.03	0.92 (88)	—	—	—
	With HP β CD	2.79 \pm 0.09 (7)	0.17 \pm 0.002	0.19 (93)	2.88 \pm 0.03 (5)	0.19 \pm 0.004	0.12 (95)
	Without HP β CD	—	—	—	—	—	—
Celecoxib	With HP β CD	2.17 \pm 0.06 (3)	0.06 \pm 0.001	0.07 (97)	2.28 \pm 0.02 (3)	0.07 \pm 0.01	0.05 (97)
	Without HP β CD	—	—	—	—	—	—
Rhodamine 6G	With HP β CD	0.91 \pm 0.05 (2)	0.02 \pm 0.001	0.03 (98)	0.96 \pm 0.06 (2)	0.02 \pm 0.002	0.02 (98)
	Without HP β CD	3.74 \pm 0.02 (2)	0.08 \pm 0.006	0.07 (98)	—	—	—

P_{app} for bovine and porcine choroid was calculated from the corresponding sclera and sclera-choroid permeabilities.

—, experiments were not performed either because of the low solubility of the solute or because of limited availability of the porcine tissue. Values in the parenthesis indicate the relative percentage resistance offered by the tissue (sclera or choroid) to the permeability of the solute across the sclera-choroid combination. For mannitol permeability across the bovine sclera-choroid-RPE preparation, the resistance offered by the sclera, choroid, and RPE layers is 39%, 20%, and 41%, respectively. The P_{app} differed significantly between the sclera and the sclera-choroid for each solute ($P < 0.05$). However, for a given solute, the P_{app} values for sclera and sclera-choroid are not significantly different between the species. P_{app} values are significantly lower in the presence of HP β CD compared with those without HP β CD.

Table 4

Tissue Partition Coefficients of Various Solutes

	Mannitol (H ³)		NaFl		Budesonide		Celecoxib		Rhodamine 6G	
	0.01 μ Ci/mL	1 μ Ci/mL	0.364 μ g/mL	36.4 μ g/mL	0.3 μ g/mL	30 μ g/mL	0.02 μ g/mL	2 μ g/mL	0.315 μ g/mL	31.45 μ g/mL
Sclera:PBS (pH 7.4)*	0.0023 \pm 0.0001	0.005 \pm 0.0004	0.656 \pm 0.020	0.64 \pm 0.03	1.20 \pm 0.30	1.24 \pm 0.40	1.391 \pm 0.50	1.48 \pm 0.003	35.13 \pm 2.30	35.97 \pm 2.49
Choroid-Bruch's layer:PBS (pH 7.4)*	0.0025 \pm 0.002	0.005 \pm 0.002	0.952 \pm 0.04	0.90 \pm 0.04	2.00 \pm 0.05	2.05 \pm 0.04	2.913 \pm 0.45	2.92 \pm 0.31	122.05 \pm 21.32	123.80 \pm 19.85
Choroid-Bruch's layer:Sclera	1.09	1.00	1.45	1.41	1.67	1.65	2.09	1.97	3.47	3.44

Data are the tissue:buffer partition coefficients or their ratios between tissues.

* Tissue partition coefficients were calculated as the ratio of solute concentration in tissue (ng/g) to solute concentration in supernatant (ng/mL) after equilibration at (37°C) for 6 hours. Solute incubations were performed without HP β CD at 37°C. Data are expressed as mean \pm SD ($n = 3$). The partition coefficients were significantly lower for sclera compared with choroid-Bruch's layer with all the solutes except mannitol. The partition coefficients were significantly different between various solutes for each tissue, except between budesonide and celecoxib in sclera.